Available online at www.sciencedirect.com

ScienceDirect

St. Petersburg Polytechnical University Journal: Physics and Mathematics 2 (2016) 201–208

www.elsevier.com/locate/spjpm

Geometric modeling of midi-fullerenes growth from C_{24} to C_{48}

Alexander I. Melker, Maria A. Krupina*

St. Petersburg State Polytechnical University, 29 Politekhnicheskaya St., St. Petersburg 195251, Russian Federation

Available online 29 July 2016

Abstract

Axonometric projections together with corresponding graphs for fullerenes are constructed in the range from 24 to 48. The growth of fullerenes is studied on the basis of the mechanism, according to which a carbon dimer embeds in a hexagon of an initial fullerene. This leads to stretching and breaking the covalent bonds which are parallel to arising tensile forces. In this case, instead of the hexagon adjoining two pentagons, one obtains two adjacent pentagons adjoining two hexagons. As a result, there arises a new atomic configuration and there is mass increase of two carbon atoms. We considered direct descendants of fullerene C_{24}; namely, C_{2n}, where $n=13$–24.

Keywords: Fullerene; Modeling; Growth; Carbon dimer; Graph; Structure.

1. Introduction

In Ref. [1], we have extended the term "fullerene" to include any convex shape inscribed into a spherical surface which can be composed of atoms, each atom having three nearest neighbors, as in usual fullerenes, whenever discussing hollow carbon clusters. This new approach allowed us to obtain possible forms of mini-fullerenes, from C_4 to C_{20}, which, in its turn, allowed filling up a gap by including in the list of fullerenes such broad-sense fullerenes.

The next step was made in Ref. [2], where the diagrams showing the forming of mini-fullerenes from single carbon atoms and carbon dimers were suggested. The diagrams have much in common for different fullerenes. In addition to the diagrams, here for the first time the graph theory was used for analysis of the fullerene structures obtained. The graph analysis provides a deep insight into both a fullerene structure and its way of forming. The graphs, similar to the formation diagrams, have also much in common for different fullerenes. Besides the graph analysis allows also solving an inverse problem, i. e., how to predict the ways of producing possible fullerenes, if their graphs are known [3]. It turned out to be possible to distinguish different families of mini-fullerenes on the graph basis and therefore to make a classification of these unusual carbon structures.

In Ref. [4], we considered the problem of fullerene growth more elaborately, namely, how to design new fullerenes and their graphs if given a basic elementary graph of a mini-fullerene playing the role of progenitor. We have developed a way of designing different families of fullerenes using such approach. As a result, we have found the family of bi-polyfoils: C_{14}, C_{18}, C_{24}, C_{30}, $C_{36;}$ the family of truncated bipyramids: C_{14}, C_{18}, C_{24} C_{30}, C_{36}; the family of cupola

* Corresponding author.
E-mail addresses: newton@imop.spbstu.ru (A.I. Melker), ksta@inbox.ru (M.A. Krupina).

http://dx.doi.org/10.1016/j.spjpm.2016.07.001

half-fullerenes: C_{10}, C_{12}, C_{16}, C_{20}, C_{24}; and the family of tetra-hexa-cell equator fullerenes: C_{20}, C_{24}, C_{32}, C_{40}, C_{48}. This classification gives not only fullerene symmetry but also connects it with its relatives.

It is worth noting that we have obtained a medium size fullerene C_{36} with D_{6h} symmetry. It was synthesized and separated from arc derived carbon soot at UC, Berkeley [5]. In literature, it is referred to as a 36-atom-carbon cage, but this name is of little value because 15 different isomers are possible [6]. Contrary to this name, our classification determines this fullerene uniquely [4]. However, some midi-fullerenes, e.g., C_{26}, C_{28} [7], were not constructed in Ref. [4], so their graphs were not known. This drawback was excluded in [8] using the graph approach developed in Refs. [2–4].

In Ref. [9], we have suggested a unified approach to drawing axonometric projections for both small and large fullerenes. In the long run, we came to the conclusion that the best way is the dimetric representation whose symmetry coincides with that of a corresponding graph. Then we have carefully studied a dimer mechanism of growing fullerenes, according to which a carbon dimer embeds either into a hexagon or a pentagon of an initial fullerene. This leads to stretching and breaking the covalent bonds which are parallel to the arising tensile forces. In the first case, instead of the hexagon adjoining two pentagons, when the dimer embeds in this hexagon, one obtains two adjacent pentagons adjoining two hexagons. In the second case, when the dimer embeds in the pentagon, two pentagons separated by a square are obtained. In both cases there arises a new atomic configuration and there is a mass increase of two carbon atoms. This process can continue until a new stable configuration is reached. In doing so, we modeled the growth of the first branch of the family of tetra-hexa-cell equator fullerenes beginning with C_{20} in the range from 20 to 36 together with some of their isomers. We have constructed the axonometric projections and the corresponding graphs for these fullerenes.

In this contribution, we consider the direct descendants of the second branch of the family of tetra-hexa-cell equator fullerenes beginning with C_{24}, namely, C_{2n}, where $n=11$–24. Our aim is to study their growth constructing at first their graphs, what is simpler, and then to develop their structure on the basis of the graphs obtained.

1.1. Tri$_2$-tetra$_3$-hexa$_9$ polyhedral fullerene C_{24}

Its atomic configuration consists of three equilateral triangles, three squares, and nine hexagons (Fig. 1) so it could be termed a tri$_2$-tetra$_3$-hexa$_9$ polyhedron. This structure together with its consistent electronic structure was obtained in Ref. [1] on the basis of a new mathematic concept of fullerenes. According to the concept, a fullerene is any shape composed of atoms, each atom having three nearest neighbors, which can be inscribed into a spherical, ellipsoidal, or similar surface close to a sphere. But what is more important, it was suggested that not only the atoms but also the shared electron pairs forming covalent bonds, were located on one and the same sphere, ellipsoid or similar surface.

1.2. Branch of tri$_2$-tetra$_3$-hexa$_9$ polyhedral fullerene C_{24}

First stage. Starting with fullerene C_{24}, one can obtain the direct descendants of this fullerene with the help of the mechanism of dimer embedding into a hexagon. Taking as a basis the structure and the graph of the fullerene we have obtained the first four fullerenes and their graphs (see Fig. 1). Here fullerenes C_{24} and C_{30} are perfect (D_{3h} symmetry), and fullerenes C_{26} and C_{28} are imperfect (C_1 symmetry). In many respects, they are similar to those of the branch generated by fullerene C_{20} [3]. To gain a better understanding of the mechanism of dimer embedding, its main features are given in the form of schematic representation (Fig. 2).

Let us analyze this figure. From the configurations shown it follows that the first embedding, which transforms fullerene C_{24} into fullerene C_{26}, deeply influences only one of the hexagons and two of its square neighbors. The hexagon transforms into two adjacent pentagons and its square neighbors become pentagons. As a result, a cluster containing four pentagons is obtained. The second imbedding transforms fullerene C_{26} into fullerene C_{28}. Similar to the previous case, one of the two remaining hexagons transforms into two adjacent pentagons, its square neighbor into a pentagon, and its pentagon neighbor into a hexagon. At last, the third embedding which leads from fullerene C_{28} to fullerene C_{30}, eliminates the last remaining hexagon and two its neighboring pentagons, but, in return, creates two adjacent pentagons and two hexagons of another local orientation,

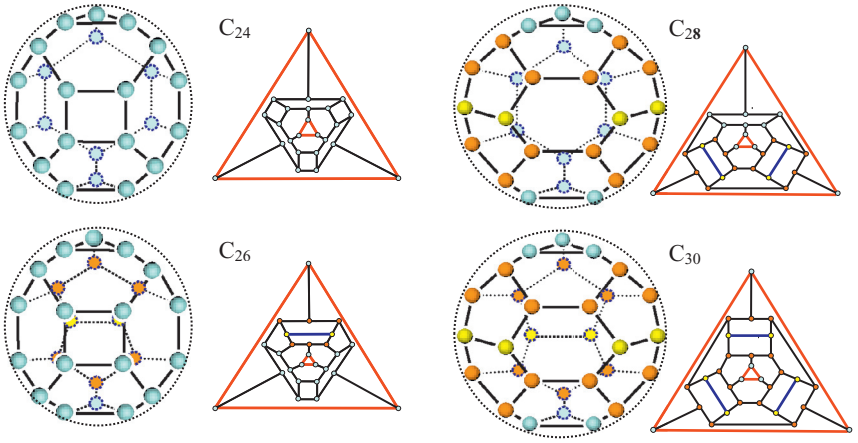

Fig. 1. Atomic structure and graphs of fullerenes C_{24}, C_{26}, C_{28}, and C_{30}.

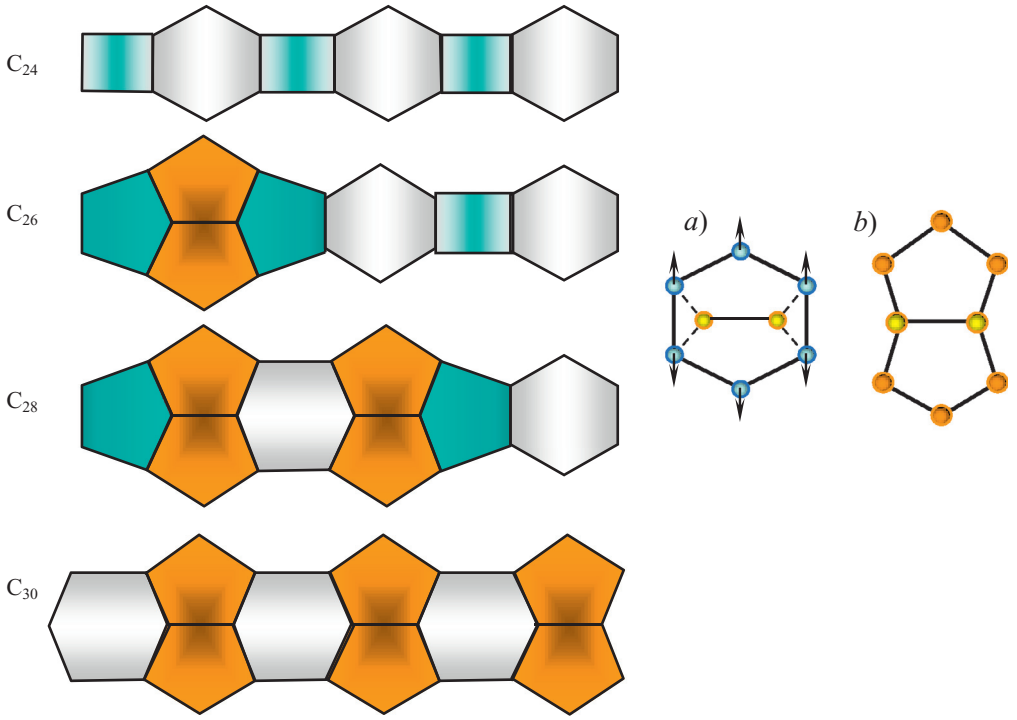

Fig. 2. Scheme reflecting the main local changes during the growth of fullerene C_{24}. Dimer embedding into a hexagon (a) which transforms into two adjacent pentagons (b).

so the hexa-octa-cell equator fullerene finally becomes a bow-tie-cell equator fullerene C_{32} (see Fig. 2), each bow tie having two bow-tie neighbors normal to it. It could be named a hexa-octa-cell equator fullerene where every two adjacent pentagons have the form of a bow tie. At the same time, in the pole areas there appear clusters composed of three adjacent hexagons with a trigon in their centers.

Second stage. The further growth of fullerene C_{30} differs from that of fullerene C_{24}. Fullerene C_{30} cannot grow in a manner similar to that of fullerene C_{24}, i.e., normal to the equator because now the equator hexagons have no neighboring pentagons oriented normal to it. However, any equator hexagon can use, for its growth, two neighboring pentagons of the equator, which are mutually antithetic. So fullerene C_{30} can continue the growth, only changing the growth direction. As a result, one obtains two imperfect fullerenes C_{32} and C_{34} with C_1 symmetry, and one perfect C_{36} with D_{3h} symmetry (Fig. 3). To gain a better

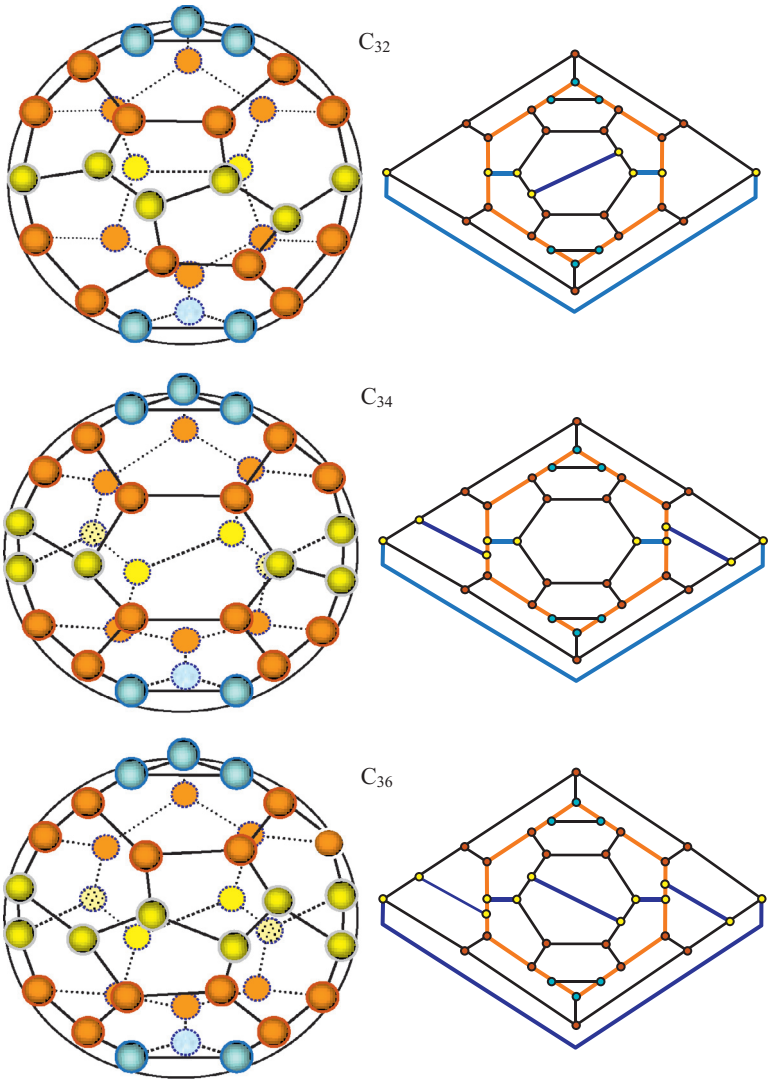

Fig. 3. Atomic structure and graphs of fullerenes C_{32}, C_{34}, and C_{36}.

understanding of the mechanism of dimer embedding, its main features are given in the form of schematic representation (Fig. 4).

The structure of fullerene C_{36} is rather interesting. For studying this fullerene it is convenient to use the system of coordinates where the axis z, or the main axis of symmetry, passes through the centers of two triangles. Each triangle surrounded by three hexagons forms a cluster. The clusters are separated by a zigzag ring of twelve atoms which create an equator. It is worth noting that all equator atoms are former dimer atoms. The fullerene is perfect, and we have the group of perfect fullerenes including C_{24}, C_{30}, and C_{36}.

Third stage. Essentially, any hexagon of fullerene C_{36} of such configuration is capable of embedding a dimer, but it will more likely embed a hexagon with not only two neighboring mutually antithetic pentagons, but one pentagon and a mutually antithetic trigon. It is connected with the well-known fact: the less is the fullerene surface, the less is its energy. A local curvature is defined by the sum of adjacent angles having a common vertex. The less is the sum, the larger is the curvature, and therefore the more is the local stress concentration. Even the first embedding of a dimer into such a hexagon increases the sum from 300 to 330º, and thus the configuration becomes more stable.

The growth of fullerene C_{36} is shown in Figs. 5–7. Among the descendants there are imperfect fullerenes C_{38}, C_{42}, and C_{46} with C_1 symmetry, semi-perfect fullerenes C_{40} (C_{1h} symmetry), C_{44} (S_2 symmetry),

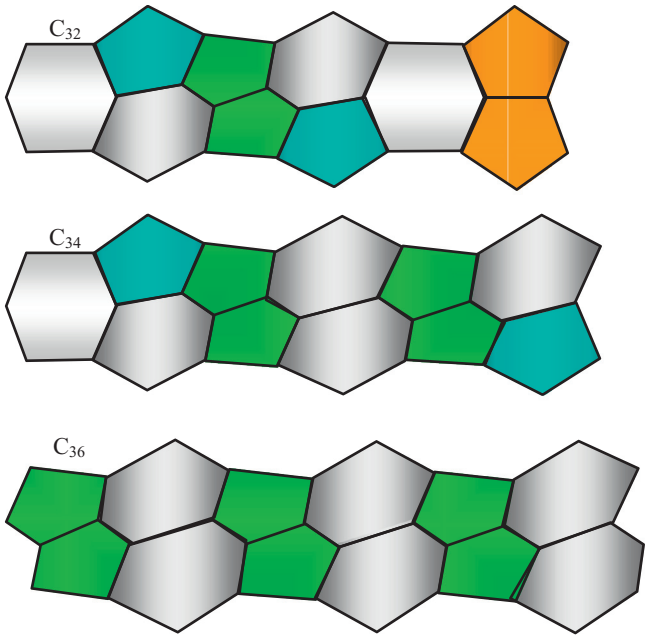

Fig. 4. Scheme reflecting the main local changes during the growth of fullerene C_{30}.

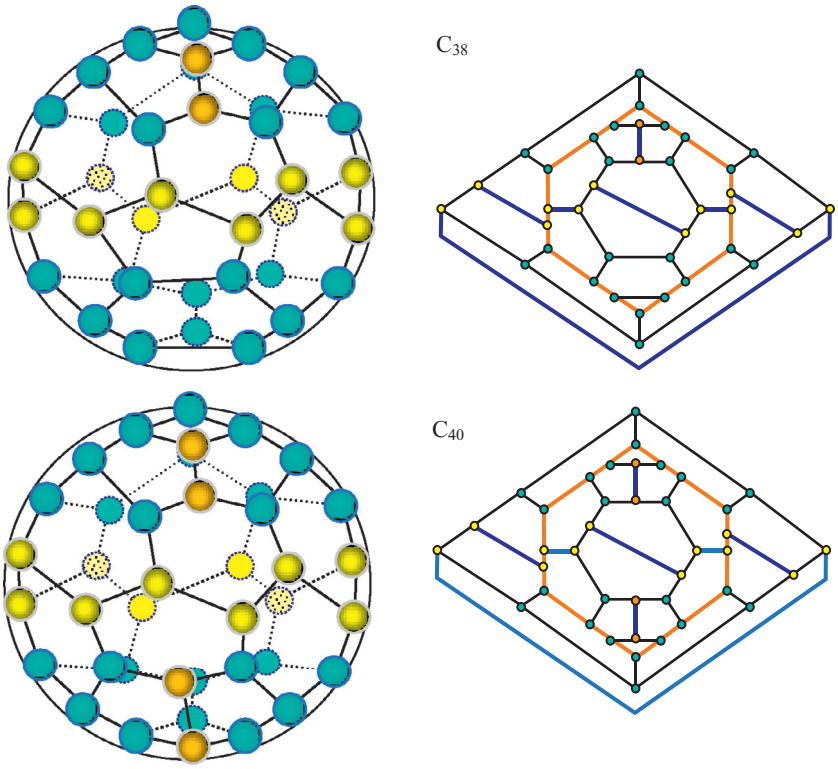

Fig. 5. Atomic structure and graphs of fullerenes C_{38} and C_{40}.

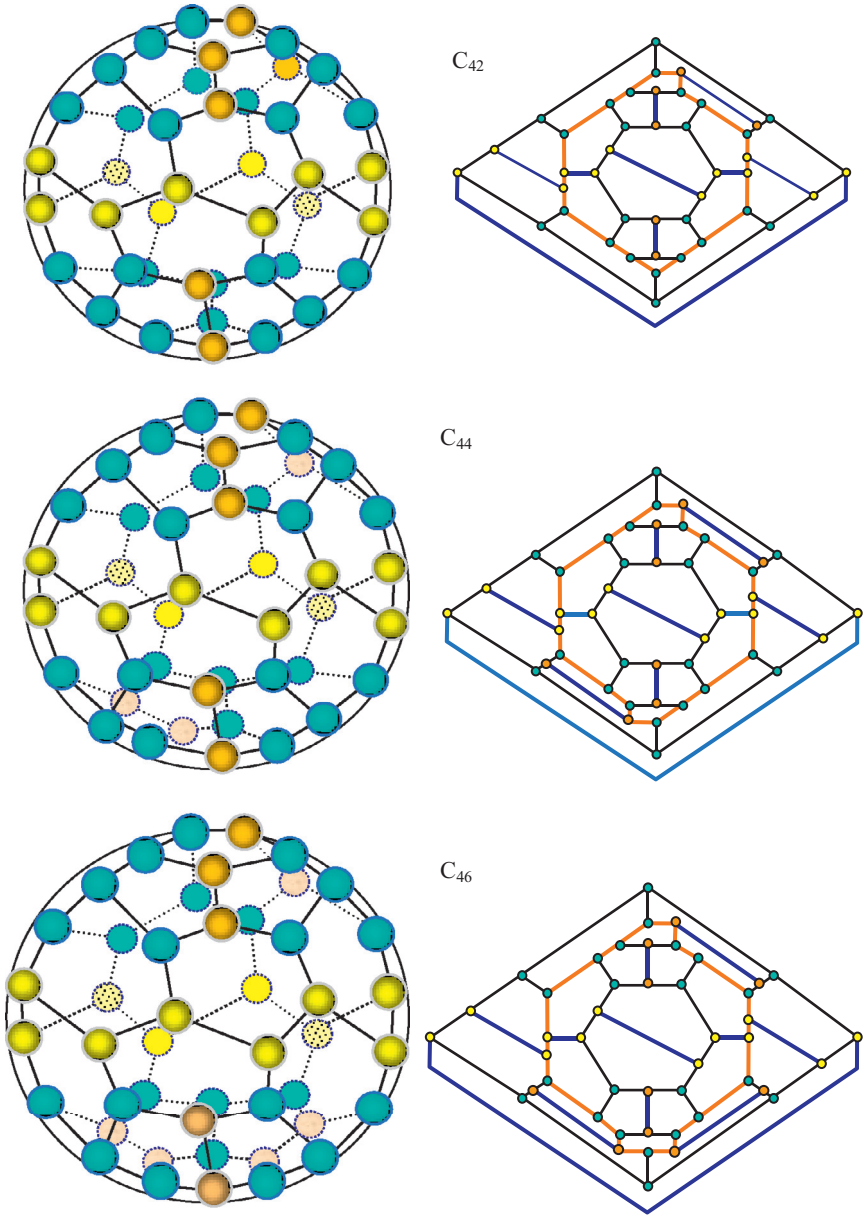

Fig. 6. Atomic structure and graphs of fullerenes C_{42}, C_{44}, and C_{46}.

and the perfect fullerene C_{48} (D_{6h} symmetry). The imperfect fullerenes have an odd number of dimers, the semi-perfect and the perfect fullerenes have an even number. The final high-symmetry fullerene C_{48} has the same structure as the fullerene C_{48} which was grown out earlier [6] from the fullerene C_{20} (Fig. 7, below). It contains clusters of eighteen atoms in the polar areas; each cluster is composed of six pentagons around a hexagon. This means that the problem of equifinality can arise here. This problem is well known in economic geography: a nucleus of towns can be different, but the final structure is the same; it has a center and outskirts.

2. Conclusion

Any calculations of fullerene energy need input data. For mini-fullerenes (up to C_{20}) the number of possible configurations is not very large, but with midi-fullerenes (C_{20}–C_{60}) a monstrous size of isomers can be obtained. It is clear that there is no big sense in studying all of them, so it is desirable to restrict

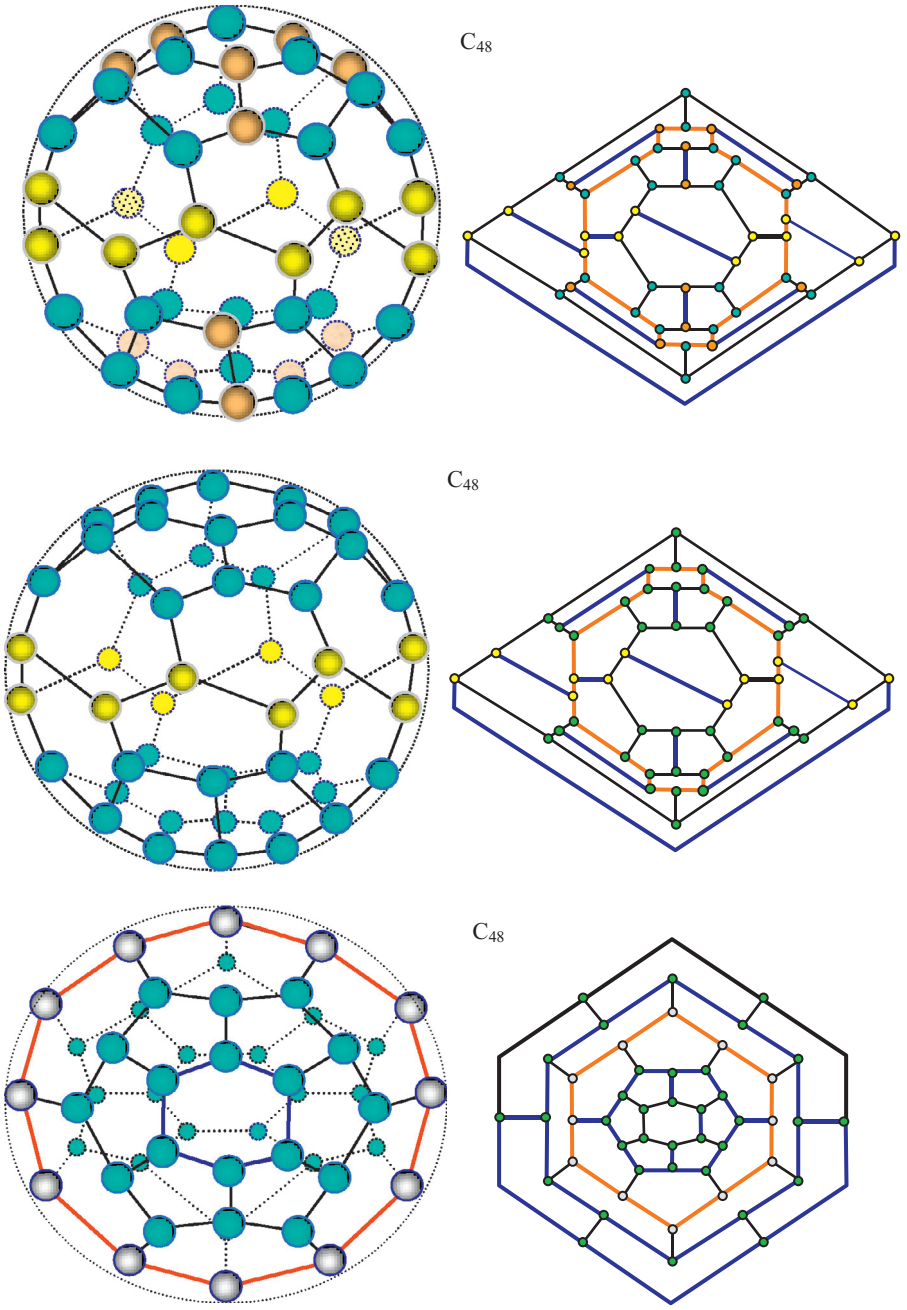

Fig. 7. Atomic structure and graphs of fullerene C_{48}. Clusters of eighteen atoms in the polar areas; each cluster containing six pentagons around a hexagon.

their number to the most stable. In this respect, geometric modeling is very useful as a first step of computer simulation for further theoretical analysis [10]. As for fullerenes, the geometric modeling is based on the principle "the minimum surface at the maximum volume". It means that a forming fullerene tends to take the form of a perfect spheroid with equal covalent bonds. We suppose that geometric modeling allows imagining from the very beginning a possible way of growing carbon clusters and thereby to decrease the number of configurations worth for studying. With the help of geometrical modeling, we have considered here the growth of fullerenes through a series of dimer imbedding reactions with initial fullerenes.

As a result, axonometric projections together with the corresponding graphs for the second branch of the family of tetra-hexa-cell equator fullerenes including some isomers are constructed in the range from 24 to 48. Some of the graphs were obtained earlier [4] but the majority is given for the first time. The process of growth of fullerenes is studied on the basis of the mechanism, according to which a carbon dimer embeds in a hexagon of an initial fullerene. This leads to stretching and breaking the covalent bonds which are parallel to the arising tensile forces. In this case, instead of the hexagon adjoining two pentagons, two adjacent pentagons adjoining two hexagons are obtained. As a result, there arises a new atomic configuration and there is a mass increase of two carbon atoms. We considered direct descendants of the second branch of the tetra-hexa-cell-equator family beginning with C_{24}, namely, C_{2n}, where $n = 13 - 24$.

Fullerenes C_{24}, C_{30}, and C_{36} can be considered to be perfect fullerenes with a threefold symmetry. The symmetry can be easily discovered looking at their graphs. The fullerenes C_{26}, C_{28}, C_{32}, and C_{34} are imperfect. By analogy with crystal physics, it can be said that the reason for imperfection is connected with the fact that the fullerenes have extra 'interstitial' dimers or 'vacant' dimers. The structure of fullerene C_{36} is rather interesting. It has two triangles around a polar axis. Each triangle surrounded by three hexagons forms a cluster. The clusters are separated by a zigzag ring of twelve atoms which create an equator. It is worth noting that all equator atoms are former dimer atoms. Although any hexagon of fullerene C_{36} is capable of embedding a dimer, but a hexagon with not only two neighboring mutually antithetic pentagons but one pentagon and a mutually antithetic trigon is more likely to do so. It is connected with the well-known fact; the less is the fullerene surface, the less is its energy. A local curvature is defined by the sum of adjacent angles having a common vertex. The less is the sum, the larger is the curvature, and therefore the more is the local stress concentration. Even the first embedding of a dimer into such a hexagon increases the sum from 300 to 330º, and thus the configuration becomes more stable.

The process of growth of fullerene C_{36} leads to forming imperfect fullerenes C_{38}, C_{42}, and C_{46}, semi-perfect fullerenes C_{40}, C_{44}, and perfect fullerene C_{48}. The imperfect fullerenes have an odd number of dimers; the semi-perfect fullerenes, as well as the perfect one, have an even number. The final high-symmetry fullerene C_{48} has the same structure as the one of fullerene C_{48} which was grown out of fullerene C_{20} [6]. It contains clusters of eighteen atoms in the polar areas; each cluster is composed of six pentagons around a hexagon. This means that there the principle of equifinality holds in this case; a nucleus of fullerenes can be different, but the final structure is the same. Therefore, the further growth of fullerene C_{48} formed in the second branch will not differ from that of the first branch.

References

[1] A.I. Melker, V. Lonch, Atomic and electronic structure of mini-fullerenes: from four to twenty, Mater. Phys. Mech. 13 (1) (2012) 22–26.
[2] A.I. Melker, Possible ways of forming mini-fullerenes and their graphs, Mater. Phys. Mech. 20 (1) (2014) 1–11.
[3] A.I. Melker, S.A. Starovoitov, T.V. Vorobyeva, Classification of mini-fullerenes on graph basis, Mater. Phys. Mech. 20 (1) (2014) 12–17.
[4] A.I. Melker, M.A. Krupina, Designing mini-fullerenes and their relatives on graph basis, Mater. Phys. Mech. 20 (1) (2014) 18–24.
[5] C. Piskoti, J. Yarger, A. Zettl, C_{36}, a new carbon solid, Nature 393 (1998) 771–774.
[6] A.M. Rao, M.S. Dresselhaus, Nanostructured forms of carbon: an overview, in: G. Benedek, P. Milani, V.G. Ralchenko (Eds.), Nanostructured Carbon for Advanced Applications, NATO Science Series II, Mathematics, Physics and Chemistry, vol. 24, Kluwer Academic Publishers, Dordrecht, 2001, pp. 3–24.
[7] G. Benedek, M. Bernasconi, D. Donadio, L. Colombo, Covalent clusters-assembled carbon solids, in: G. Benedek, P. Milani, V.G. Ralchenko (Eds.), Nanostructured Carbon for Advanced Applications, NATO Science Series II, Mathematics, Physics and Chemistry, vol. 24, Kluwer Academic Publishers, Dordrecht, 2001, pp. 89–126.
[8] M.A. Krupina, A.I. Melker, S.A. Starovoitov, T.V. Vorobyeva, Structure and graphs of midi-fullerenes, in: Proceedings of the International Workshop on New Approaches to High-Tech: Nano-Design, Technology, Computer Simulations, NDTCS' 2015, 16, 2015, pp. 23–26.
[9] A.I. Melker, Growth of midi-fullerenes from twenty to sixty, in: Proceedings of the International Workshop on New Approaches to High-Tech: Nano-Design, Technology, Computer Simulations, NDTCS' 2015, 16, 2015, pp. 34–37.
[10] A.I. Melker, Dynamics of Condensed Matter, St. Petersburg Academy of Sciences on Strength Problems, St. Petersburg, 2010, p. 342. Vol. 2, Collisions and Branchings.